



Proceeding Paper

Total Neutron Cross-Section Measurement on CH with a Novel 3D-Projection Scintillator Detector [†]

Ciro Riccio ^{1,*} , Anushka Agarwal ², Howard Budd ³, Jordi Capó ⁴, Pooi Chong ², Georgios Christodoulou ⁵, Mikhail Danilov ⁶, Anna Dergacheva ⁷ , Albert De Roeck ⁵, Neha Dokania ¹, Dana Douqa ⁸, Katherine Dugas ⁹, Sergei Fedotov ⁷, Sunwoo Gwon ¹⁰, Ryan Howell ³, Konosuke Iwamoto ¹¹, Cesar Jesús-Valls ⁴, Chang Kee Jung ¹, Siva Prasad Kasetti ⁹, Marat Khabibullin ⁷, Alexey Khotjantsev ⁷, Tatsuya Kikawa ¹², Umüt Kose ⁵, Yuri Kudenko ^{7,13,14} , Soichiro Kuribayashi ¹², Thomas Kutter ⁹, David Last ², Shih-Kai Lin ⁹, Thorsten Lux ⁴ , Steven Manly ³ , David A. Martinez Caicedo ¹⁵, Sergei Martynenko ¹, Tsunayuki Matsubara ¹⁶, Christopher Mauger ², Kevin McFarland ³, Clark McGrew ¹, Aleksandr Mefodiev ⁷, Oleg Mineev ⁷, Takeshi Nakadaira ¹⁶, Etam Noah ⁸, Andrew Olivier ³, Vittorio Paolone ¹⁷, Sandro Palestini ⁵ , Alexander Paul-Torres ⁹, Rachel Pellegrino ², Manuel Alejandro Ramírez ², Jairo Rodriguez Rondon ¹⁵, Federico Sanchez ⁸, Davide Sgalaberna ¹⁸, Wilf Shorrock ^{19,†}, Andriasetta Sitiraka ¹⁵, Kim Siyeon ¹⁰, Nataliya Skrobova ⁶ , Sergey Suvorov ⁷, Abraham Teklu ¹, Martin Tzanov ⁹, Yoshi Uchida ¹⁹, Clarence Wret ³, Guang Yang ^{1,§}, Nikolay Yershov ⁷, Masashi Yokoyama ¹¹ and Perri Zilberman ¹

- ¹ Department Physics and Astronomy, State University of New York at Stony Brook, Stony Brook, NY 11794, USA; neha.dokania@stonybrook.edu (N.D.); chang.jung@stonybrook.edu (C.K.J.); sergey.martynenko@stonybrook.edu (S.M.); clark.mcgreg@stonybrook.edu (C.M.); abraham.teklu@stonybrook.edu (A.T.); gyang9@berkeley.edu (G.Y.); perri.zilberman@stonybrook.edu (P.Z.)
- ² Department of Physics and Astronomy, University of Pennsylvania, Philadelphia, PA 19104, USA; anushkaagarwal521@gmail.com (A.A.); eric0722@sas.upenn.edu (P.C.); dlast@sas.upenn.edu (D.L.); cmauger@sas.upenn.edu (C.M.); rachpell@sas.upenn.edu (R.P.); alex0402@sas.upenn.edu (M.A.R.)
- ³ Department of Physics and Astronomy, University of Rochester, Rochester, NY 14627, USA; hbudd@fnal.gov (H.B.); rhowell3@ur.rochester.edu (R.H.); steven.manly@rochester.edu (S.M.); kevin@rochester.edu (K.M.); aolivier@ur.rochester.edu (A.O.); c.wret@rochester.edu (C.W.)
- ⁴ Institut de Física d'Altes Energies (IFAE), The Barcelona Institute of Science and Technology, 08193 Bellaterra, Barcelona, Spain; jcapo@ifae.es (J.C.); cjesus@ifae.es (C.J.-V.); thorsten.lux@ifae.es (T.L.)
- ⁵ CERN European Organization for Nuclear Research, 1211 Geneva, Switzerland; georgios.christodoulou@cern.ch (G.C.); deroeck@mail.cern.ch (A.D.R.); umut.kose@cern.ch (U.K.); sandro.palestini@cern.ch (S.P.)
- ⁶ Lebedev Physical Institute of the Russian Academy of Sciences, Moscow 119991, Russia; danilov@lebedev.ru (M.D.); skrobovana@lebedev.ru (N.S.)
- ⁷ Institute for Nuclear Research of the Russian Academy of Sciences, Moscow 115191, Russia; dergacheva@inr.ru (A.D.); sergei.fedotov@cern.ch (S.F.); marat@inr.ru (M.K.); alex@inr.ru (A.K.); kudenko@inr.ru (Y.K.); mefodiev@inr.ru (A.M.); oleg@inr.ru (O.M.); suvorov@inr.ru (S.S.); yershov@inr.ru (N.Y.)
- ⁸ Département de Physique Nucléaire et Corpusculaire, University of Geneva, 1205 Geneva, Switzerland; dana.douqa@unige.ch (D.D.); etamnoah@gmail.com (E.N.); federico.sanchezNieto@unige.ch (F.S.)
- ⁹ Department of Physics and Astronomy, Louisiana State University, Baton Rouge, LA 70803, USA; kduga14@lsu.edu (K.D.); kasetti@phys.lsu.edu (S.P.K.); kutter@lsu.edu (T.K.); shihkailin1@lsu.edu (S.-K.L.); apault1@lsu.edu (A.P.-T.); mtzanov@lsu.edu (M.T.)
- ¹⁰ High-Energy Physics Center, Chung-Ang University, 84 Heukseok-ro, Dongjak-gu, Seoul 06974, Republic of Korea; tnsdn302@naver.com (S.G.); siyeon@cau.ac.kr (K.S.);
- ¹¹ Department of Physics, University of Tokyo, Tokyo 113-0033, Japan; kiwamoto@hep.phys.s.u-tokyo.ac.jp (K.I.); masashi@phys.s.u-tokyo.ac.jp (M.Y.)
- ¹² Department of Physics, Kyoto University, Kyoto 606-8502, Japan; kikawa.tatsuya.6e@kyoto-u.ac.jp (T.K.); kuribayashi.soichiro.57u@st.kyoto-u.ac.jp (S.K.)
- ¹³ Moscow Institute of Engineering and Physics (MEPhI), Moscow 115409, Russia
- ¹⁴ Moscow Institute of Physics and Technology (MIPT), Moscow 141701, Russia
- ¹⁵ South Dakota School of Mines and Technology, Rapid City, SD 57701, USA; david.martinezcaicedo@sdsmt.edu (D.A.M.C.); jairohernan.rodriguezrondon@mines.sdsmt.edu (J.R.R.); andriasetasitiraka@gmail.com (A.S.)
- ¹⁶ High Energy Accelerator Research Organization (KEK), Tsukuba 305-0801, Japan; tsuna@post.kek.jp (T.M.); nakadair@neutrino.kek.jp (T.N.)



Citation: Riccio, C.; Agarwal, A.; Budd, H.; Capó, J.; Chong, P.; Christodoulou, G.; Danilov, M.; Dergacheva, A.; De Roeck, A.; Dokania, N.; et al. Total Neutron Cross-Section Measurement on CH with a Novel 3D-Projection Scintillator Detector. *Phys. Sci. Forum* **2023**, *8*, 29. <https://doi.org/10.3390/psf2023008029>

Academic Editor: Yue Zhao

Published: 1 August 2023



Copyright: © 2023 by the authors. Licensee MDPI, Basel, Switzerland. This article is an open access article distributed under the terms and conditions of the Creative Commons Attribution (CC BY) license (<https://creativecommons.org/licenses/by/4.0/>).

¹⁷ Department of Physics and Astronomy, University of Pittsburgh, Pittsburgh, PA 15260, USA; paolonepitt@gmail.com

¹⁸ Institute for Particle Physics and Astrophysics, ETH Zurich, 8093 Zurich, Switzerland; davide.sgalaberna@cern.ch

¹⁹ Department of Physics, Imperial College London, London SW7 2AZ, UK; w.shorrock17@imperial.ac.uk (W.S.); yoshi.uchida@imperial.ac.uk (Y.U.)

* Correspondence: ciro.riccio@stonybrook.edu

† Presented at the 23rd International Workshop on Neutrinos from Accelerators, Salt Lake City, UT, USA, 30–31 July 2022.

‡ Current address: Department of Physics and Astronomy, University of Sussex, Brighton BN1 9RH, UK.

§ Current address: Department of Physics, University of California, Berkeley, Berkeley, CA 94720, USA.

Abstract: Long-baseline neutrino oscillation experiments rely on detailed models of neutrino interactions on nuclei. These models constitute an important source of systematic uncertainty, partially because detectors to date have been unable to detect final state neutrons. A novel three-dimensional projection scintillator tracker will be a component of the upgraded off-axis near detector of the T2K experiment. Due to the good timing resolution and fine granularity, this technology is capable of measuring neutron kinematics in neutrino interactions on an event-by-event basis and will provide valuable data for refining neutrino interaction models. A prototype is exposed to the neutron beamline at Los Alamos National Laboratory with neutron energies between 0 and 800 MeV. In order to demonstrate the capability to measure neutron kinematics, the total neutron–scintillator cross section as a function of the neutron kinetic energy is measured.

Keywords: neutron kinematics; neutrino oscillation; long-baseline neutrino oscillation experiment; SuperFGD; T2K

1. Introduction

A novel 3D-projection scintillator detector, called Super Fine Grained Detector (SuperFGD), will be the tracker of the upgraded off-axis near detector of T2K, ND280 [1]. Currently under construction, it is a highly segmented scintillator detector made of 1 cm optically isolated cubes read by three wavelength-shifting fibers (WLS). The light yield is detected by a multi-pixel photon counter (MPPC). It has close to two million cubes of 10 mm with $1920 \times 560 \times 1840 \text{ mm}^3$ volume. The SuperFGD setup enhances capabilities for measuring leptons and hadrons resulting from neutrino interactions by providing pseudo-3D reconstruction with full solid angle acceptance and lower energy thresholds. Among the different improvements it promises is the detection of neutrons created in (anti)neutrino interactions and the measurement of their kinematics on an event-by-event basis. Thanks to its good timing resolution and fine granularity, the neutron kinematics can be measured using its time of flight (ToF) and the distance it traveled before interacting (lever arm). A schematic representation of the quantities employed to measure neutron kinematics is shown in Figure 1.

Neutron kinematics is one of the missing pieces for (anti)neutrino energy reconstruction in long-baseline (LBL) neutrino oscillation experiments but is not currently accessible for detectors employed in such experiments. Future LBL experiments have as one of their goals the measurement of the parameter governing the charge and parity symmetry (δ_{CP}) that requires a precision measurement of the shape of the neutrino energy spectrum. Therefore, the measurement of neutron kinematics is needed to increase its precision. The possibility to measure neutron kinematics opens new ways to investigate neutrino–nucleus interactions and, in particular, the nuclear effects involved [2].

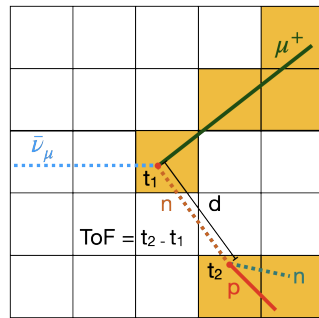


Figure 1. Representation of a muon antineutrino interaction producing a positively charged muon and a neutron at time t_1 . The neutron then interacts with a nucleus of the detector material and produces a proton and another neutron at time t_2 . The ToF is given by the difference in time between the two interactions, and the distance (d) is the lever arm. Each square represents a single scintillator cube, and the lines represent true particle trajectories. This figure was adapted from Ref. [2].

2. Experimental Setup

For the characterization of the response of SuperFGD to neutrons, we exposed a prototype made of $24 \times 8 \times 48$ cubes of 10 mm (SuperFGD prototype) to the neutron beam provided by the Los Alamos Neutron Science Center (LANSCE) at the Los Alamos National Laboratory (LANL). The prototype was initially built to test the scintillator cube assembly method and to characterize the detector response to charged particles, exposing it to the beam provided by the CERN Proton Synchrotron facility. The result of the analysis of the data taken showed very good performance: an average light yield around 58 photoelectrons (p.e.) per minimum ionizing particle, 3% cross-talk, a time resolution of 1.1 ns for a single channel, and very good particle identification [3].

The neutron beam has an energy range between 0 and 800 MeV. It is made by employing a proton beam composed of sub-nanosecond wide proton bunches separated by $1.8 \mu\text{s}$ that impinge on a tungsten target. The interactions produce neutrons and photons, which travel to the detector. Two collimators, one located near the target and another one located before the detector, help to collimate the beam. Photons arrive before the neutron, for which the ToF is determined by measuring their arrival times relative to the flux of photons. The SuperFGD prototype was located 90 m from the beam production point. This distance, along with the measured ToF, is used to measure the neutron kinetic energy. The detector was oriented such that the neutron beam (z -direction) was parallel to the longest dimension. As a result of the analysis of the data taken in 2019, we measured the total neutron cross section on hydrocarbon. This result represents the first measurement achieved with the technology introduced by SuperFGD.

3. Cross-Section Extraction Strategy

In order to extract the total cross-section measurement on CH, we use the so-called extinction method [4]. The neutron flux decreases as a function of depth in the detector due to neutron interactions, and the attenuation decreases exponentially along the z -coordinate according to the following formula:

$$N(z) = N_0 e^{-T\sigma_{\text{tot}}z}, \quad (1)$$

where N_0 is the initial neutron event rate, and $N(z)$ is the event rate at the reconstructed z position. T ($T = (\rho_{\text{CH}} \times N_{\text{Avogadro}}) / m_{\text{CH}} = 4.623 \times 10^{22} \text{ nucleons/cm}^3$) and σ_{tot} are the nuclear density and the neutron total cross section, respectively. The cross section for different neutron kinetic energy bins can be extracted by fitting the event rate distribution along z using the exponential function in Equation (1). The event rate attenuation can be measured by choosing a particular event topology and measuring the change in its rate as a function of depth in the detector. We assume that the fraction of the total cross section extracted from the chosen topology does not change as a function of the depth. We choose

to select events with a single reconstructed track since the vertex can be reconstructed more clearly and a good sample purity can be achieved.

3.1. Event Reconstruction and Selection

For the event reconstruction, we consider only events that occur within a certain time window, which is specified by the flux of photons. Then, we require more than 3 hits per event and more than 20 p.e. per hit, and by hit, we mean the signal recorded by each MPPC. After that, we group the cluster in time; if consecutive hits are within 17.5 ns, they belong to the same cluster. Only events with one time cluster are selected to reduce pile-up. We proceed with building voxels (3-dimensional pixels), combining the three 2D-views of the detector. After forming the voxels, we group them using the density-based spatial clustering of applications with noise (DBSCAN) algorithm. To select single-track events we reject those that have more than one spatial cluster. We select only events with more than three voxels, which is the minimum number to define a track and less than eight voxels to reduce the dependence on the detector acceptance. We perform cuts on three variables defined using the eigenvectors and eigenvalues computed performing a principle component analysis (PCA) of the matrix associated with the cluster. The matrix is defined as follows:

$$M_{ij} = \sum_{ij} \frac{(\vec{v} - \vec{c})_i (\vec{v} - \vec{c})_j}{N}, \quad (2)$$

where N is the number of voxels in the cluster, \vec{v} is the vector associated with a voxel in the cluster and \vec{c} is the center of the cluster. Using the first (λ_1) and second (λ_2) eigenvalues, we compute the variable $L = (\lambda_1 - \lambda_2) / \lambda_1$ and require it to be larger than 0.7. To improve the selection of track-like events, we compute the projected distance between one voxel and the center of mass of the cluster on the second principal vector. We calculate the distance between the 2 voxels furthest away from each other, and we require this quantity to be lower than 1.4 cm. Then, we consider the principal vector that defines the direction of the best-fit 3-dimensional line of the cluster. We take as the origin the center of the first voxel in z . We compute the distance between each voxel and this best-fit line. If the maximum distance is larger than 1.2 cm, the event is rejected. Finally, we identify the vertex to be the first voxel in z and we require it to be within $1.5 \times 1.5 \text{ cm}^2$ around the beam center and its z position to be between 1 and 40 cm. The first layer is removed to reduce the background due to interactions in the material upstream the detector, as well as the last eight layers to mitigate the impact of the limited detector size.

3.2. Fitting and Systematic Uncertainties

For the extraction of the cross section, we build the distribution of the number of events as a function of the depth for different neutron energy bins. The energy is computed using the ToF of the neutron, and the binning is optimized, taking into account the time resolution and statistics. The energy is restricted to be between 98 and 688 MeV. Events below 98 MeV do not result in clusters long enough to form tracks, above 688 MeV, the statistics are limited. We fit every distribution with the exponential function of Equation (1), where the coefficient $T\sigma_{\text{tot}}$ is a free parameter.

The systematic uncertainties affecting our measurements are as follows:

- Detector uncertainty, which is due mainly to detector non-uniformity and misalignment between cubes. It is estimated computing the ratio between the number of single-track events and the number of events just with more than 20 p.e. per hit.
- Uncertainty due to invisible scattering, i.e., all the scattering that either produced neutrons only or did not deposit enough energy, and the primary vertex is missed. It is estimated by tuning the transverse spread of the beam in a Monte Carlo (MC) simulation to match the one observed in the data.
- Uncertainty associated with geometric acceptance, i.e., how the limited detector size affects the selected number of events. It is evaluated looking at the variation of the

number of events in the case where detector size in the z-direction is smaller. Its impact is reduced, requiring the number of voxels per event to be less than 8 and considering only events with vertex with $1 < z < 40$ cm.

- Uncertainty due to light yield variation for each channel, which is measured using cosmic ray data.
- Uncertainty on time resolution, which is measured using the photons flux and data taken during charged particle beam tests at CERN [3].
- Collimator interactions: events interacting inside the collimators before entering the detector can lose energy and cause a bias in the energy estimation. It is evaluated looking at the energy loss by neutrons inside the collimators in a dedicated MC simulation.

The first four uncertainties change the number of events in each z-layer, while the last two change the kinetic energy estimation. For the first group of uncertainties, we vary the number of events according to a Gaussian distribution with the number of events in each energy bin and z-layer as the mean and the estimated systematic uncertainty as the standard deviation. This results in a new event distribution as a function of the vertex position that we fit with the exponential function in Equation (1). This procedure is repeated one thousand times, and the error on the cross section is given by the width of the distribution of the cross section extracted from every variation. In the second group, what is varied is the energy, and then a new distribution of the number of events as a function of the z-layer is fitted for every variation. The error on the cross section is then extracted as for the first group. The statistical uncertainty is given by the square root of the number of events in every energy bin and z-layer. The total uncertainty is the sum in quadrature of the single uncertainties.

The total neutron cross section as a function of the kinetic energy is extracted using a total of 20 h of data, and the impact of each uncertainty is shown in Figure 2. The statistical error is small compared with systematic uncertainties, for which the dominant one is the detector uncertainty, which is between ~ 8 and $\sim 14\%$. The measured cross section is in agreement within the uncertainty with the reconstructed GEANT4 [5] prediction obtained using the QGSP_BERT physics list, and the energy-integrated (98–688 MeV) cross section is 0.36 ± 0.05 barn with a $\chi^2/\text{d.o.f.}$ of 22.03/38.

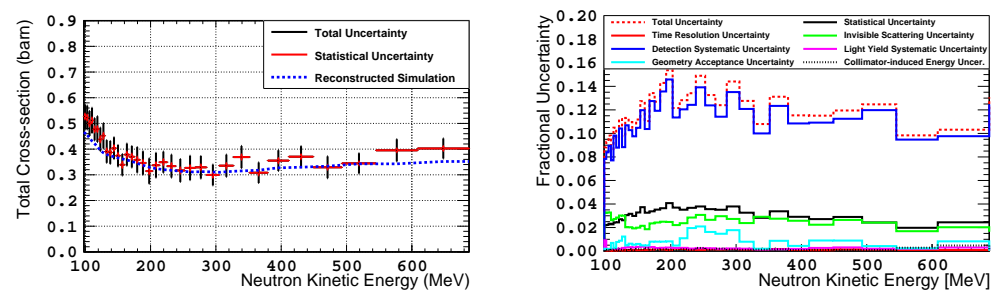


Figure 2. (Left) total neutron cross section as a function of the kinetic energy. Black error bars represent the total uncertainty and red bars the statistical uncertainty. The cross section is compared with reconstructed GEANT4 prediction obtained using the QGSP_BERT physics list (blue dotted line). (Right) Relative uncertainty on the neutron cross section as a function of the kinetic energy. Different colors correspond to different sources of uncertainty.

4. Conclusions

SuperFGD is a novel 3D-projection scintillator detector that will be the tracker of the upgraded off-axis near detector of T2K, ND280. Among various improvements, there is the detection of neutrons created in (anti)neutrino interactions and the measurement of their kinematics on an event-by-event basis. In this work, we present the total neutron cross section on hydrocarbon. This result represents the first measurement achieved with the technology introduced by SuperFGD. More details about this analysis can be found in Ref. [6]. Other data were collected in December 2020 at LANL, employing both the

SuperFGD prototype and another prototype built within a collaboration between Japanese and US institutions. Different configurations of the two detectors were used to study different features of neutron interactions, and analysis is ongoing.

Author Contributions: The authors contributed equally to this work. All authors have read and agreed to the published version of the manuscript.

Funding: This work was performed, in part, at the Los Alamos Neutron Science Center (LANSCE), a NNSA User Facility operated for the U.S. Department of Energy (DOE) by Los Alamos National Laboratory (Contract 89233218CNA000001). We thank Keegan Kelly for technical support throughout the experiment and analysis. This work was supported by JSPS KAKENHI Grant Numbers JP26247034, JP16H06288, and JP20H00149. This work was supported in part by the RSF grant No. 19-12-00325 and by the MHES (Russia) grant “Neutrino and astroparticle physics” No. 075-15-2020-778. We acknowledge funding from the Spanish Ministerio de Economía y Competitividad (SEIDI-MINECO) under Grants No. PID2019-107564GB-I00. IFAE is partially funded by the CERCA program of the Generalitat de Catalunya. We acknowledge the Swiss National Foundation through grant No. 200021 85012. We further acknowledge the U.S.–Japan Science and Technology Cooperation Program in High Energy Physics, the support of the US Department of Energy, Office of High Energy Physics and the support from the University of Pennsylvania.

Institutional Review Board Statement: Not applicable.

Informed Consent Statement: Not applicable.

Data Availability Statement: The data release and the explanation of its content are available <https://arxiv.org/src/2207.02685v3/anc/> (accessed on 8 June 2023).

Conflicts of Interest: The authors declare no conflict of interest.

References

1. Abe, K.; Aihara, H.; Ajmi, A.; Andreopoulos, C.; Antonova, M.; Aoki, S.; Asada, Y.; Ashida, Y.; Atherton, A.; Atkin, E.; et al. T2K ND280 Upgrade—Technical Design Report. *arXiv* **2019**, arXiv:1901.03750.
2. Munteanu, L.; Suvorov, S.; Dolan, S.; Sgalaberna, D.; Bolognesi, S.; Manly, S.; Yang, G.; Giganti, C.; Jesús-Valls, C. New method for an improved antineutrino energy reconstruction with charged-current interactions in next-generation detectors. *Phys. Rev. D* **2020**, *101*, 092003. [[CrossRef](#)]
3. Blondel, A.; Bogomilov, M.; Bordoni, S.; Cadoux, F.; Douqa, D.; Dugas, K.; Ekelof, T.; Favre, Y.; Fedotov, S.; Fransson, K.; et al. The SuperFGD Prototype Charged Particle Beam Tests. *J. Inst.* **2020**, *15*, P12003. [[CrossRef](#)]
4. Bhandari, B.; Bian, J.; Bilton, K.; Callahan, C.; Chaves, J.; Chen, H.; Cline, D.; Cooper, R.L.; Danielson, D.; Danielson, J.; et al. First Measurement of the Total Neutron Cross Section on Argon between 100 and 800 MeV. *Phys. Rev. Lett.* **2019**, *123*, 042502. [[CrossRef](#)] [[PubMed](#)]
5. Agostinelli, S.; Allison, J.; Amako, K.A.; Apostolakis, J.; Araujo, H.; Arce, P.; Asai, M.; Axen, D.; Banerjee, S.; Barrand, G.J.; et al. GEANT4—A simulation toolkit. *Nucl. Instrum. Meth. Sect. A* **2003**, *506*, 250–303. [[CrossRef](#)]
6. Agarwal, A.; Budd, H.; Capó, J.; Chong, P.; Christodoulou, G.; Danilov, M.; Dergacheva, A.; De Roeck, A.; Dokania, N.; Douqa, D.; et al. Total neutron cross-section measurement on CH with a novel 3D-projection scintillator detector. *Phys. Lett. B* **2023**, *840*, 137843. [[CrossRef](#)]

Disclaimer/Publisher’s Note: The statements, opinions and data contained in all publications are solely those of the individual author(s) and contributor(s) and not of MDPI and/or the editor(s). MDPI and/or the editor(s) disclaim responsibility for any injury to people or property resulting from any ideas, methods, instructions or products referred to in the content.